Organic LETTERS

Letter

pubs.acs.org/OrgLett

Rh-Mediated Enantioselective Synthesis, Crystal Structures, and Photophysical/Chiroptical Properties of Phenanthrenol-Based [9]Helicene-like Molecules

Ryota Yamano,[†] Jun Hara,[§] Koichi Murayama,[†] Haruki Sugiyama,[‡] Kota Teraoka,[‡] Hidehiro Uekusa,[‡] Susumu Kawauchi,[†] Yu Shibata,[†] and Ken Tanaka*[,†,§]

[†]Department of Chemical Science and Engineering and [‡]Department of Chemistry, Tokyo Institute of Technology, O-okayama, Meguro-ku, Tokyo 152-8550, Japan

[§]Department of Applied Chemistry, Graduate School of Engineering, Tokyo University of Agriculture and Technology, Koganei, Tokyo 184-8588, Japan

Supporting Information

ABSTRACT: The enantioselective synthesis of phenanthrenol-based [9]-helicene-like molecules has been achieved via the rhodium-mediated intramolecular [2 + 2 + 2] cycloadditions of 3-phenanthrenol-linked triynes. Crystal structures and photophysical/chiroptical properties of these [9]-helicene-like molecules were compared with the corresponding [7]helicene-like molecules.

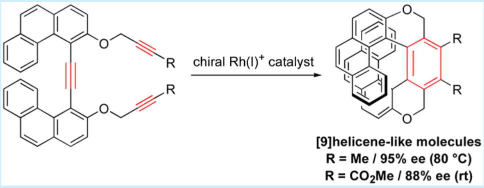

The enantioselective synthesis of higher order helicenes and helicene-like molecules is a challenging target in organic synthesis due to the difficulty of overcoming steric barriers as well as controlling enantioselectivity in annulation.[1] For this purpose, the transition-metal-catalyzed enantioselective aromatic ring construction has been applied to their catalytic enantioselective synthesis.[2−9] Specifically, the transition-metal-catalyzed [2 + 2 + 2] cycloaddition of alkynes has been extensively applied to this synthesis.[2−6,8] However, the enantioselective synthesis of helicenes and helicene-like molecules, possessing more than eight consecutive rings, has been reported in a limited number of examples.[3b,e,8a] In 2007, our research group achieved the enantioselective synthesis of [7]helicene-like molecules **2a** and **2b** with good ee values by the rhodium(I)-catalyzed intramolecular [2 + 2 + 2] cycloaddition of 2-naphthol-linked triynes **1a** and **1b**, respectively (Scheme 1, top).[3a] Subsequently, the double [2 + 2 + 2] cycloadditions of naphthol-linked tetraynes with 1,4-diynes[3b] and a 2-naphthol-linked hexayne[3e] enabled the enantioselective synthesis of [9]- and [11]helicene-like molecules, respectively. Although the use of 3-phenanthrenol-linked triynes, tetraynes, and hexaynes in the above-mentioned synthesis would enable the enantioselective synthesis of [9]-, [11]-, and [13]helicene-like molecules, respectively, the method for the synthesis of 3-phenanthrenol-linked oligoynes has not been developed. In this paper, we efficiently synthesized the 3-phenanthrenol-linked triynes **1c** and **1d**, and the rhodium(I)-mediated intramolecular [2 + 2 + 2] cycloaddition of them enabled the enantioselective synthesis of [9]helicene-like molecules **2c** and **2d** with higher ee values than **2a** and **2b** (Scheme 1, bottom). Crystal structures and photophysical/chiroptical properties of **2c** and **2d** are also disclosed and compared with those of previously synthesized **2a** and **2b**.

Scheme 1

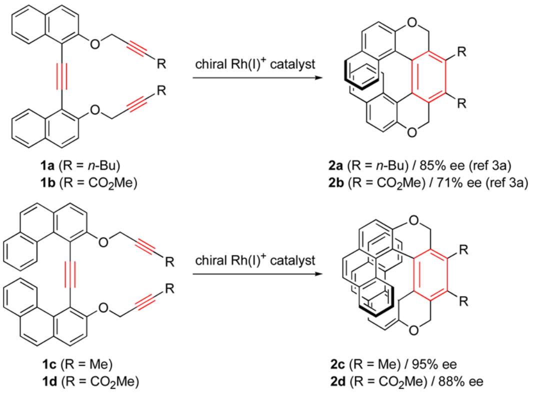

The 3-phenanthrenol-linked triynes **1c** and **1d** were prepared starting from commercially available 2,6-dimethoxybromobenzene (**3**) as shown in Scheme 2. Demethylation of **3** with BBr$_3$ afforded phenol **4**. Triflation of **4** followed by the palladium-catalyzed Suzuki−Miyaura cross-coupling with boronic acid **5** afforded biaryl **6**. Desilylation of **6** afforded terminal alkyne **7**, and the subsequent platinum-catalyzed intramolecular hydroarylation of **7** gave 4-bromo-3-methoxyphenanthrene (**8**). The palladium-catalyzed decarboxylative double-Sonogashira coupling with propiolic acid[10] afforded internal alkyne **9**. Demethylation of **9** with lithium diphenylphosphide[11] provided acetylene-linked bis(3-phenanthrenol) **10**. Propargylation of **10** with 1-bromo-2-butyne afforded electron-rich triyne **1c**, and propargylation of **10** with propargyl bromide followed by the

Received: November 1, 2016

DOI: 10.1021/acs.orglett.6b03279

Scheme 2

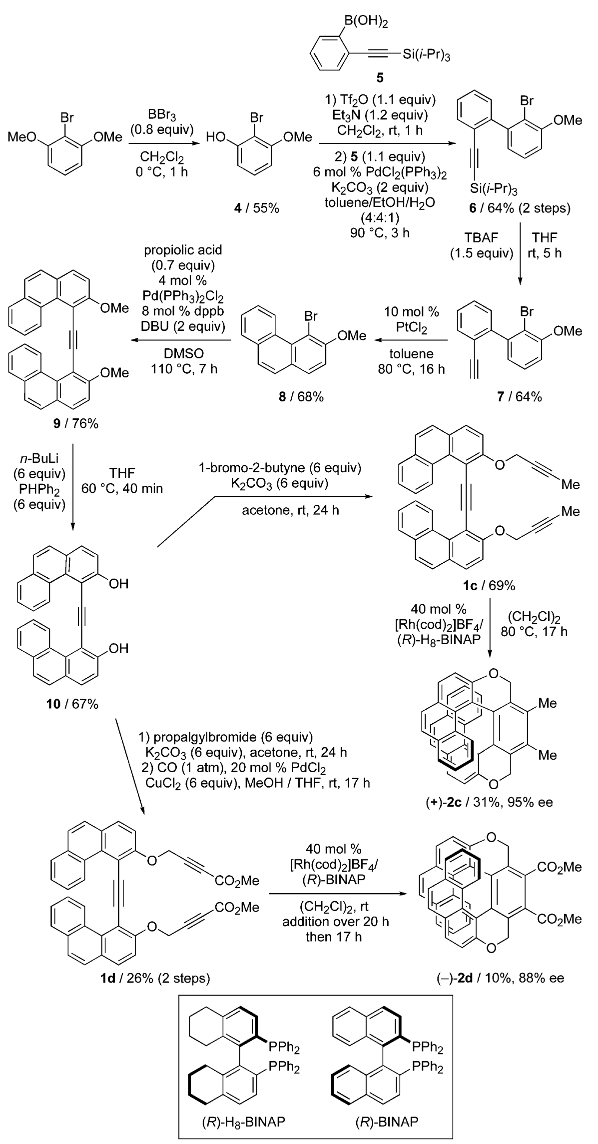

palladium-catalyzed methoxycarbonylation with CO and methanol[12] afforded electron-deficient triyne **1d**.

Pleasingly, the enantioselective intramolecular [2 + 2 + 2] cycloaddition of **1c** proceeded at 80 °C in the presence of a cationic rhodium(I)/(*R*)-H$_8$−BINAP catalyst to give [9]-helicene-like molecule (+)-**2c** in 31% yield with 95% ee.[13] In the case of **1d**, the desired cycloaddition proceeded at room temperature in the presence of a cationic rhodium(I)/(*R*)-BINAP catalyst to give [9]helicene-like molecule (−)-**2d** with 88% ee, although the yield was low (10%).[13] These reactions did not afford the previously reported formal [2 + 1 + 2 + 1] cycloaddition products[3a] but instead provided complex mixtures of byproducts other than **2c** and **2d**.

The enantiopure crystals of (−)-**2d** were readily obtained by recrystallization of enantioenriched (−)-**2d** (88% ee) from ethanol. The crystal structure of (−)-**2d** is shown in Figure 1. As shown in the top view (Figure 1a, left), two phenanthrene moieties are completely overlapped. As shown in the side view (Figure 1a, right), two phenanthrene moieties were almost flat despite the large steric hindrance. The presence of two flexible −CH$_2$O− moieties in the molecule releases the steric strain. As shown in Figure 1b, the helically chiral molecules are stacked along the *a*-axis in the unit cell to form continuous chiral helical columns. Phenanthrene moieties are almost parallel and face each other in the column. The distances of two phenanthrene moieties in the molecule and between two individual molecules are very close (3.72 and 3.99 Å, respectively, Figure 1b, left). These features are driven from intermolecular π−π stacking of phenanthrene moieties and C−H···O interaction between methylene hydrogen and carbonyl oxygen. On the other hand, previously reported [7]helicene-like molecule (−)-**2b** also forms continuous chiral helical columns; however, the distance for two naphthalene moieties between two individual molecules (8.04 Å, Figure 1b, right) is much longer than that of two naphthalene moieties in the molecule (3.89 Å).[3a] Stronger intermolecular π−π stacking of phenanthrene moieties than naphthalene moieties results in the closer packing of **2d** than **2b**. Recrystallization of enantioenriched (+)-**2c** (95% ee) was also attempted. Unfortunately, however, racemic crystals of **2c** preferentially grown and did not form continuous helical columns (Figure S1).[14]

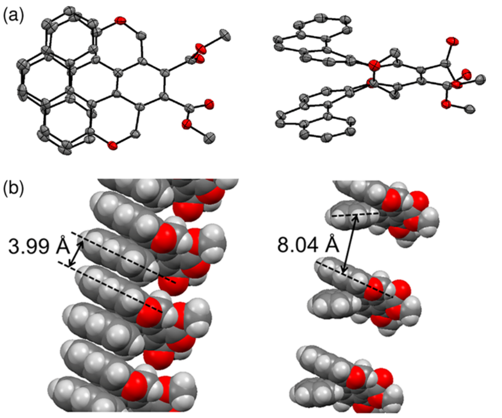

Figure 1. X-ray crystallographic analysis of [9]helicene-like molecule (−)-**2d** with ellipsoids at 50% probability. (a) Left: top view, right: side view. (b) Packing model [left: (−)-**2d**, right: (−)-**2b** (ref 3a)].

Photophysical properties of [9]helicene-like molecules **2c** and **2d** were compared with [7]helicene-like molecules **2a** and **2b** (Table 1, Figure 2a,b, and Figure S2a,S2b[14]). [9]Helicene-like molecules **2c** and **2d** showed red shifts of absorption and emission maxima compared with [7]helicene-like molecules **2a** and **2b**, respectively. The shape of the emission spectra of **2d** did not change in high concentration (1.0 × 10^{-3} M) despite its dense packing in the crystalline state. Quantum yields of **2c** and **2d** in CHCl$_3$ solution were lower than those of **2a** and **2b**, respectively. Compared with other known [9]helicenes, the quantum yield of **2c** was lower than that of a [9]helicene-like molecule bearing four pyran rings (ϕ_F = 0.10)[3e] but higher than all-benzenoid [9]helicene (ϕ_F = 0.01).[16a]

Table 1. Photophysical Properties of [7]- and [9]Helicene-like Molecules[a]

compd	UV absorption λ_{max}/nm	fluorescence λ_{max}/nm (excitation wavelength/nm)	ϕ_F (excitation wavelength/nm)
2a	358[b]	435 (380)[b]	0.27 (380)
2b	380[b]	479 (380)[b]	0.23 (380)
2c	375	483 (420)	0.05 (420)
2d	388	514 (420)	0.18 (420)

[a] Measured in CHCl$_3$ at 25 °C at 1.0 × 10^{-5} M. [b] Data for ref 3a.

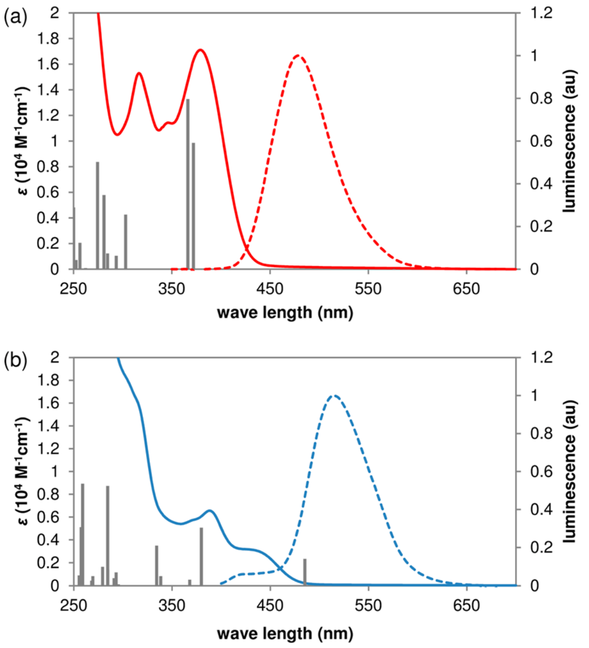

Figure 2. (a) UV/vis absorption (solid line) and emission (dashed line) spectra of **2b** in $CHCl_3$ (1.0×10^{-5} M). (b) UV/vis absorption (solid line) and emission (dashed line) spectra of **2d** in $CHCl_3$ (1.0×10^{-5} M). The gray lines show the UV/vis absorption spectrum calculated by the TD-DFT method at the wB97XD/6-311G(d) level.

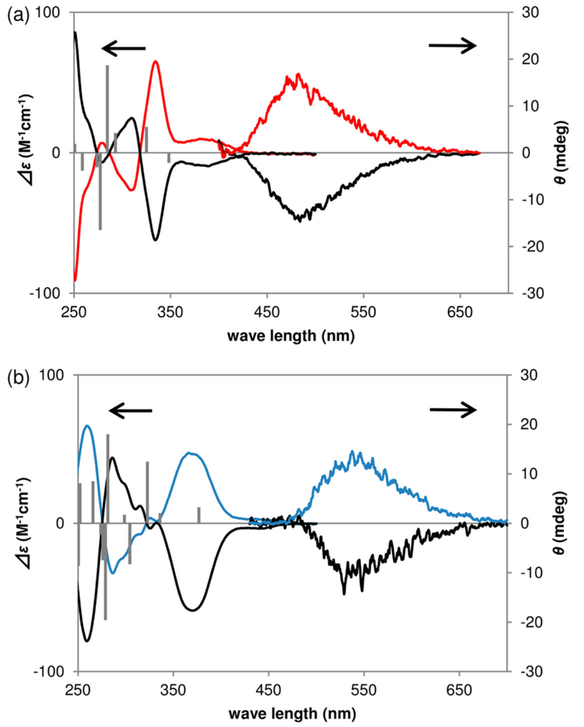

Figure 3. (a) ECD and CPL spectra of (+)-**2b** (blue) and (−)-**2b** (black) in $CHCl_3$ (2.0×10^{-5} M). (b) ECD and CPL spectra of (+)-**2d** (red) and (−)-**2d** (black) in $CHCl_3$ (2.0×10^{-5} M). The gray lines show the CD spectrum for (*P*)-**2b** and (*P*)-**2d** calculated by the TD-DFT method at the wB97XD/6-311G(d) level.

Finally, we examined the structure−chiroptical property relationship of [7]- and [9]helicene-like molecules **2a−d** (Table 2, Figure 3a,b, and Figure S3a,S3b[14]). We found that the electronic circular dichroism (ECD) spectra of (+)-**2a−d** and (−)-**2a−d** in chloroform exhibit mirror-image relationships. Calculation of the UV/vis absorption and CD spectra of (+)-**2b** and **2d** revealed that the longest peak has a large contribution of the transition between HOMO and LUMO. The HOMO localized on the phenanthrene moieties and the LUMO localized on the benzene ring bonded carbonyl groups (Figure S4). We also conducted circularly polarized luminescence (CPL) measurements (differential emission of right circularly polarized light versus left circularly polarized light in chiral molecular systems) of [7]- and [9]helicene-like molecules **2b** and **2d** in chloroform. [9]Helicene-like molecule **2d** exhibited CPL activity as the CPL spectra of (+)- and (−)-helicene-like molecules are mirror images. The degree of CPL is given by the luminescence dissymmetry ratio, which is defined as $g_{\text{lum}} = 2(I_L - I_R)/(I_L + I_R)$, where I_L and I_R are the luminescence intensities of left and right circularly polarized light.[15] The value of the [9]helicene-like molecule **2d** was larger than that of [7]helicene-like molecule **2b**.[16] Similarly, the optical rotation values, which are converted into the values of 100% ee, of **2c** and **2d** were larger than those of **2a** and **2b**. Compared with other known [9]helicenes, the optical rotation value of **2c** was smaller than that of all-benzenoid [9]helicene ($[\alpha]^{25}_D$ = 8100)[16b] but larger than that for a [9]helicene-like molecule bearing four pyran rings ($[\alpha]^{25}_D$ = 1228).[3e]

Table 2. Chiroptical Properties of [7]- and [9]Helicene-Like Molecules[a]

compd	$[\alpha]^{25}_D$ [b]	$g_{\text{lum}} = 2(I_L - I_R)/(I_L + I_R)$ [b,c] (wavelength/nm)[d]
2a	710[e]	
2b	1280[e]	9.5×10^{-4} (473)
2c	2020	
2d	1440	1.1×10^{-3} (547)

[a] Measured in $CHCl_3$ at 25 °C. [b] Values are calculated as 100% ee. [c] At 2.0×10^{-5} M. [d] Excited at 350 nm. [e] Data of ref 3a.

In conclusion, we have achieved the enantioselective synthesis of phenanthrenol-based [9]helicene-like molecules via rhodium-mediated intramolecular [2 + 2 + 2] cycloadditions of 3-phenanthrenol-linked triynes. X-ray crystallographic analysis of [9]helicene-like molecule (−)-**2d**, possessing the phthalate moiety, revealed that the densely packed continuous chiral helical columns are formed in the crystals through strong intermolecular π−π stacking of phenanthrene moieties. Structure−photophysical and chiroptical property relationships in [7]- and [9]helicene-like molecules have also been examined, which revealed that larger the size of helicene-like molecules increases the optical rotation value and anisotropy factor (*g*) of CPL. Future works will include the enantioselective synthesis of [11]- and [13]helicene-like molecules via rhodium-catalyzed double [2 + 2 + 2] cycloadditions using 3-phenanthrenol-linked tetraynes and hexaynes, respectively.

■ ASSOCIATED CONTENT

Ⓢ Supporting Information

The Supporting Information is available free of charge on the ACS Publications website at DOI: 10.1021/acs.orglett.6b03279.

Experimental procedures and compound characterization data (PDF)
X-ray crystallographic data for (+)-**2c** (CIF)
X-ray crystallographic data for (−)-**2d** (CIF)

AUTHOR INFORMATION

Corresponding Author

*E-mail: ktanaka@apc.titech.ac.jp.

ORCID

Ken Tanaka: 0000-0003-0534-7559

Notes

The authors declare no competing financial interest.

ACKNOWLEDGMENTS

This work was supported in part by ACT-C from JST (Japan) and a Grant-in-Aid for Scientific Research (No. 26102004) from MEXT (Japan). We thank the Natural Science Center for Basic Research and Development (N-BARD), Hiroshima University, for the measurement of CPL using JASCO CPL-200 and Prof. Toshikazu Takata and Dr. Kazuko Nakazono (Tokyo Institute of Technology) for the measurement of ECD. We also thank Takasago International Corporation for the gift of H_8-BINAP and Segphos, Umicore for generous support in supplying the rhodium and palladium complexes, and Central Glass Co., Ltd., for the gift of trifluoromethanesulfonic anhydride.

REFERENCES

(1) For reviews, see: (a) Tanaka, K.; Kimura, Y.; Murayama, K. *Bull. Chem. Soc. Jpn.* **2015**, *88*, 375. (b) *Transition-Metal-Mediated Aromatic Ring Construction*; Tanaka, K., Ed.; Wiley: Hoboken, 2013; Chapter 10. (c) Peng, Z.; Takenaka, N. *Chem. Rec.* **2013**, *13*, 28. (d) Shen, Y.; Chen, C.-F. *Chem. Rev.* **2012**, *112*, 1463. (e) Amemiya, R.; Yamaguchi, M. *Chem. Rec.* **2008**, *8*, 116. (f) Rajca, A.; Miyasaka, M. In *Functional Organic Materials: Syntheses, Strategies, and Applications*; Müller, T. T. J., Bunz, U. H. F., Eds.; Wiley-VCH: Weinheim, 2007; p 543. (g) Nuckolls, C.; Shao, R.; Jang, W.-G.; Clark, N. A.; Walba, D. M.; Katz, T. J. *Chem. Mater.* **2002**, *14*, 773. (h) Katz, T. J. *Angew. Chem., Int. Ed.* **2000**, *39*, 1921.

(2) For a review, see: *Transition-Metal-Mediated Aromatic Ring Construction*; Tanaka, K., Ed.; Wiley: Hoboken, 2013.

(3) For the rhodium(I) catalysis, see: (a) Tanaka, K.; Kamisawa, A.; Suda, T.; Noguchi, K.; Hirano, M. *J. Am. Chem. Soc.* **2007**, *129*, 12078. (b) Tanaka, K.; Fukawa, N.; Suda, T.; Noguchi, K. *Angew. Chem., Int. Ed.* **2009**, *48*, 5470. (c) Fukawa, N.; Osaka, T.; Noguchi, K.; Tanaka, K. *Org. Lett.* **2010**, *12*, 1324. (d) Sawada, Y.; Furumi, S.; Takai, A.; Takeuchi, M.; Noguchi, K.; Tanaka, K. *J. Am. Chem. Soc.* **2012**, *134*, 4080. (e) Kimura, Y.; Fukawa, N.; Miyauchi, Y.; Noguchi, K.; Tanaka, K. *Angew. Chem., Int. Ed.* **2014**, *53*, 8480. (f) Murayama, K.; Oike, Y.; Furumi, S.; Takeuchi, M.; Noguchi, K.; Tanaka, K. *Eur. J. Org. Chem.* **2015**, *2015*, 1409.

(4) For nickel(0) catalysis, see: (a) Stará, I. G.; Starý, I.; Kollárovič, A.; Teplý, F.; Vyskočil, Š.; Šaman, D. *Tetrahedron Lett.* **1999**, *40*, 1993. (b) Teplý, F.; Stará, I. G.; Starý, I.; Kollárovič, A.; Šaman, D.; Vyskočil, Š.; Fiedler, P. *J. Org. Chem.* **2003**, *68*, 5193. (c) Jančařik, A.; Rybáček, J.; Cocq, K.; Chocholoušová, J. V.; Vacek, J.; Pohl, R.; Bednárová, L.; Fiedler, P.; Cisařová, I.; Stará, I. G.; Starý, I. *Angew. Chem., Int. Ed.* **2013**, *52*, 9970. (d) Buchta, M.; Rybácek, J.; Jančařík, A.; Kudale, A. A.; Buděšínský, M.; Chocholoušová, J. V.; Vacek, J.; Bednárová, L.; Císařová, I.; Bodwell, G. J.; Starý, I.; Stará, I. G. *Chem. - Eur. J.* **2015**, *21*, 8910.

(5) For iridium(I) catalysis, see: Shibata, T.; Uchiyama, T.; Yoshinami, Y.; Takayasu, S.; Tsuchikama, K.; Endo, K. *Chem. Commun.* **2012**, *48*, 1311.

(6) For cobalt(I) catalysis, see: (a) Heller, B.; Hapke, M.; Fischer, C.; Andronova, A.; Starý, I.; Stará, I. G. *J. Organomet. Chem.* **2013**, *723*, 98. (b) Klívar, J.; Jančařík, A.; Šaman, D.; Pohl, R.; Fiedler, P.; Bednárová, L.; Starý, I.; Stará, I. G. *Chem. - Eur. J.* **2016**, *22*, 14401.

(7) For other recent examples of the enantioselective synthesis of helicenes and helicene-like molecules, see: (a) Sako, M.; Takeuchi, Y.; Tsujihara, T.; Kodera, J.; Kawano, T.; Takizawa, S.; Sasai, H. *J. Am. Chem. Soc.* **2016**, *138*, 11481. (b) Tanaka, M.; Shibata, Y.; Nakamura, K.; Teraoka, K.; Uekusa, H.; Nakazono, K.; Takata, T.; Tanaka, K. *Chem. - Eur. J.* **2016**, *22*, 14190. (c) Doulcet, J.; Stephenson, G. R. *Chem. - Eur. J.* **2015**, *21*, 18677. (d) Doulcet, J.; Stephenson, G. R. *Chem. - Eur. J.* **2015**, *21*, 13431. (e) Nakamura, K.; Furumi, S.; Takeuchi, M.; Shibuya, T.; Tanaka, K. *J. Am. Chem. Soc.* **2014**, *136*, 5555. (f) Kötzner, L.; Webber, M. J.; Martínez, A.; DeFusco, C.; List, B. *Angew. Chem., Int. Ed.* **2014**, *53*, 5202. (g) Grandbois, A.; Collins, S. K. *Chem. - Eur. J.* **2008**, *14*, 9323. (h) Caeiro, J.; Peña, D.; Cobas, A.; Pérez, D.; Guitián, E. *Adv. Synth. Catal.* **2006**, *348*, 2466. (i) Miyasaka, M.; Rajca, A.; Pink, M.; Rajca, S. *J. Am. Chem. Soc.* **2005**, *127*, 13806. (j) Carreño, M. C.; González-López, M.; Urbano, A. *Chem. Commun.* **2005**, 611. (k) Rajca, A.; Miyasaka, M.; Pink, M.; Wang, H.; Rajca, S. *J. Am. Chem. Soc.* **2004**, *126*, 15211. (l) Carreño, M.C.; García-Cerrada, S.; Urbano, A. *Chem. - Eur. J.* **2003**, *9*, 4118.

(8) For the asymmetric synthesis of helicenes and helicene-like molecules via diastereoselective [2 + 2 + 2] cycloaddition, see: (a) Sehnal, P.; Stará, I. G.; Šaman, D.; Tichý, M.; Míšek, J.; Cvačka, J.; Rulíšek, L.; Chocholoušová, J.; Vacek, J.; Goryl, G.; Szymonski, M.; Císařová, I.; Starý, I. *Proc. Natl. Acad. Sci. U. S. A.* **2009**, *106*, 13169. (b) Sámal, M.; Chercheja, S.; Rybácek, J.; Chocholousova, J. V.; Vacek, J.; Bednárova, L.; Saman, D.; Stará, I. G.; Starý, I. *J. Am. Chem. Soc.* **2015**, *137*, 8469.

(9) For other recent examples of the diastereoselective synthesis of helicenes and helicene-like molecules, see: (a) Kaneko, E.; Matsumoto, Y.; Kamikawa, K. *Chem. - Eur. J.* **2013**, *19*, 11837. (b) Lin, A.; Dou, G.-L.; Hu, M.-H.; Cao, C.-P.; Huang, Z.-B.; Shi, D.-Q. *Org. Lett.* **2013**, *15*, 1238.

(10) Park, K.; Bae, G.; Moon, J.; Choe, J.; Song, K.; Lee, S. *J. Org. Chem.* **2010**, *75*, 6244.

(11) (a) Ireland, R. E.; Walba, D. M. *Org. Synth.* **1977**, *56*, 44. (b) Arichi, N.; Hata, K.; Takemoto, Y.; Yamada, K.; Yamaoka, Y.; Takasu, K. *Tetrahedron* **2015**, *71*, 233.

(12) Tsuji, J.; Takahashi, M.; Takahashi, T. *Tetrahedron Lett.* **1980**, *21*, 849.

(13) For the optimization of reaction conditions for **1c** and **1d**, see Tables S1 and S2 in the Supporting Information.

(14) See the Supporting Information.

(15) For selected recent examples of CPL of a small organic molecular system, see: (a) Alnoman, R. B.; Rihn, S.; O'Connor, D. C.; Black, F. A.; Costello, B.; Waddell, P. G.; Clegg, W.; Peacock, R. D.; Herrebout, W.; Knight, J. G.; Hall, M. J. *Chem. - Eur. J.* **2016**, *22*, 93. (b) Gon, M.; Morisaki, Y.; Sawada, R.; Chujo, Y. *Chem. - Eur. J.* **2016**, *22*, 2291. (c) Sakai, H.; Kubota, T.; Yuasa, J.; Araki, Y.; Sakanoue, T.; Takenobu, T.; Wada, T.; Kawai, T.; Hasobe, T. *J. Phys. Chem. C* **2016**, *120*, 7860. (d) Goto, K.; Yamaguchi, R.; Hiroto, S.; Ueno, H.; Kawai, T.; Shinokubo, H. *Angew. Chem., Int. Ed.* **2012**, *51*, 10333. (e) Maeda, H.; Bando, Y.; Shimomura, K.; Yamada, I.; Naito, M.; Nobusawa, K.; Tsumatori, H.; Kawai, T. *J. Am. Chem. Soc.* **2011**, *133*, 9266. (f) Kaseyama, T.; Furumi, S.; Zhang, X.; Tanaka, K.; Takeuchi, M. *Angew. Chem., Int. Ed.* **2011**, *50*, 3684. (g) Tsumatori, H.; Nakashima, T.; Kawai, T. *Org. Lett.* **2010**, *12*, 2362. See also refs 3d and 7e.

(16) (a) Vander Donckt, E. V.; Nasielski, J.; Greenleaf, J. R.; Birks, J. B. *Chem. Phys. Lett.* **1968**, *2*, 409. (b) Martin, R. H.; Marchant, M. J. *Tetrahedron* **1974**, *30*, 343.

DOI: 10.1021/acs.orglett.6b03279
Org. Lett. XXXX, XXX, XXX−XXX